

Laminated $\text{Ti}_3\text{SiC}_2/\text{Zr}$ based composites obtained by spark plasma sintering

E P Sedanova¹, T L Murashkina¹, D G Krotkevich¹, Y R Mingazova¹, A M Lider¹ and N Travitzky^{1,2}

¹National Research Tomsk Polytechnic University, 634050 Tomsk, Russia

²Friedrich-Alexander-Universität Erlangen-Nürnberg, Erlangen, Germany

E-mail: eps4@tpu.ru

Abstract. This paper is devoted to the fabrication of laminated $\text{Ti}_3\text{SiC}_2/\text{Zr}$ based composites from Ti_3SiC_2 filled preceramic paper and Zr powder. The composites represented a “layers-by-layer” structure and were sintered by spark plasma at 1400 °C and 50 MPa for 10-30 min. The densification behavior during the sintering, microstructure of obtained composites and influence of the holding time on the phase composition were studied.

1. Introduction

MAX-phases are relatively new class of heat-resistant materials with a unique combination of metal and ceramic properties, such as heat resistance, high modulus of elasticity, oxidation resistance, thermal conductivity, and machinability. The MAX-phase Ti_3SiC_2 demonstrates high values of mechanical and thermodynamic properties that causes great interest in this material for industry [1-4]. Spark plasma sintering (SPS) is widely used for MAX-phase synthesis, because this method has huge potential for the fabrication of dense materials in a relatively short time, at lower temperature, and with improved mechanical properties compared to traditional hot isostatic pressing and other compaction methods [5].

Previous studies [6, 7, 8] have shown the possibility of spark plasma sintering of Ti_3SiC_2 -based composites using a several-layer stack of preceramic papers filled with Ti_3SiC_2 powder. It was shown that the use of preceramic papers (90 wt.% of powder filler) as a feedstock for SPS makes it possible to obtain dense composites with a flexural strength of more than 600 MPa in a short sintering cycle. The multilayer approach can be used to obtain laminated composites to improve their mechanical properties and create gradient structures by alternating layers of paper with other materials [9].

The aim of this research was to obtain laminated $\text{Ti}_3\text{SiC}_2/\text{Zr}$ -based composites and analyze phase composition and microstructure of obtained materials.

2. Materials and Methods

2.1. Sample preparation and sintering procedure

The preceramic paper with Ti_3SiC_2 powder filler (90 wt.%) and pure Zr powder (99,95 %) was used as starting materials. The fabrication of preceramic papers is clearly described in [10]. The paper sheets were cut into disks with a diameter of 12.5 mm and thickness of approximately 300 μm . The feedstock for sintering was compiled by “layer-by-layer” stacking of paper disks and Zr powder, as shown on Fig.1. The average particle size of Zr powder was 30 μm . The composites were obtained by spark plasma sintering using SPS 10-4 (Advanced Technology, USA). A stack of preceramic paper and Zr powder



Content from this work may be used under the terms of the [Creative Commons Attribution 3.0 licence](https://creativecommons.org/licenses/by/3.0/). Any further distribution of this work must maintain attribution to the author(s) and the title of the work, journal citation and DOI.

layers was placed between two graphite punches. Graphite foil was inserted between graphite die and sintered material to ensure good conductivity and prevent the reaction of sintering materials with graphite tools.

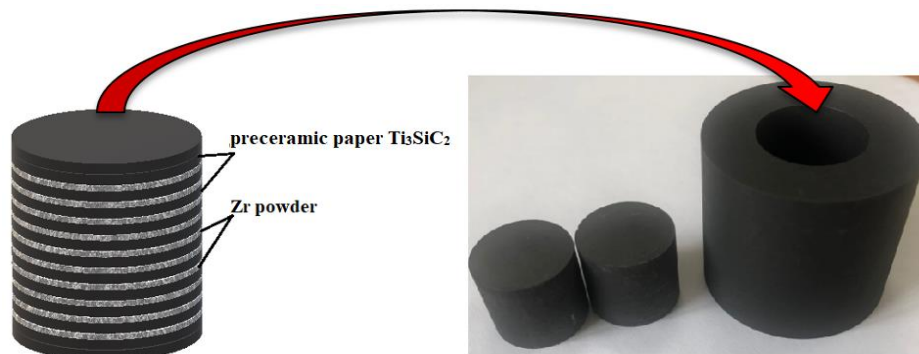


Figure 1. Schematic representation of feedstock processing process.

The sintering was performed in vacuum. The composites were sintered at the temperature of 1400 °C, pressure of 50 MPa and holding time of 10-30 min.

2.2. Characterization

Phase composition was analyzed by X-ray diffraction using Shimadzu XRD 7000S diffractometer (CuK_α radiation) equipped with OneSight high-speed 1280-channel detector. Surface microstructure of the materials was studied by scanning electron microscopy (SEM) using Vega 3 (TESCAN, Czech Republic) microscope, equipped with energy-dispersive microscopy (EDX) attachment. The samples were preliminary grinded and polished using SiC papers (ISO markings from 60 to 2000) and diamond suspensions with a grain size of up to 6 μm .

3. Results and Discussion

3.1. Densification behavior

To study the kinetic processes during the sintering of composites, the shrinkage, temperature, pressure, and current passed through the graphite tooling depending on the sintering time were analyzed. The densification behavior of the composite based on $\text{Ti}_3\text{SiC}_2/\text{Zr}$ sintered at a temperature of 1400 °C under pressure of 50 MPa for 10 minutes is shown in Figure 2. The shrinkage value of materials was determined as the displacement of the graphite punches system relative to the position of the system before the start of heating.

The sintering process occurs in several stages due to deformations caused by thermal and mechanical impacts on the material. The first stage (I) corresponds to the mechanical deformation of the composite due to the applied pressure and the beginning of passing a current through the graphite tooling and the feedstock. The second stage (II) corresponds to the decomposition of the organic component in preceramic papers and the removal of adsorbed gases from the surface of the graphite tooling and the entire volume of the sample. Stage three (III) - deformation caused by heating the material to the sintering temperature. When a certain temperature is reached (the beginning of sintering), the process of sample compaction starts. Stage four (IV) corresponds to isothermal holding for a certain time. In this case, the compaction process is the main. The final stage (V) is the process of recrystallization of the material when it is cooled. A sharp increase in shrinkage is caused by the reverse process of thermal expansion (compression of the material).

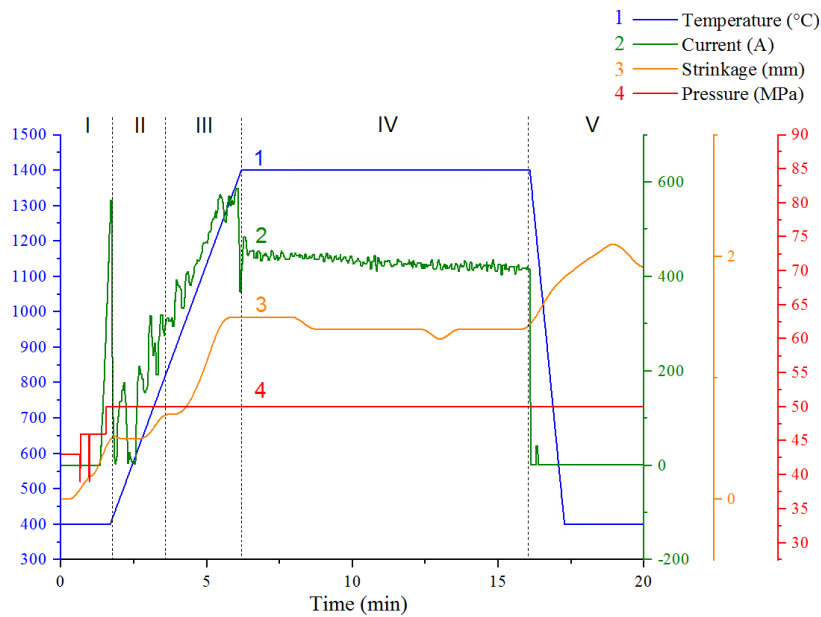


Figure 2. Densification behavior of composite based on Ti_3SiC_2/Zr sintered at a temperature of 1400 °C under pressure of 50 MPa for 10 minutes.

For Ti_3SiC_2/Zr composites sintered for 10 min, the compaction of the material over the entire SPS cycle was 54%. With an increase in the duration of isothermal holding to 30 min, the shrinkage value of the material increases to 65%.

3.2. Crystalline structure

The analysis of XRD data of the composites based on Ti_3SiC_2 and Ti_3SiC_2/Zr sintered by SPS are shown in Figure 3 and in Table 1. The structure of composites formed from preceramic paper is represented by Ti_3SiC_2 , TiC, and Al_2O_3 phases. The structure of composites formed from preceramic paper with the addition of zirconium is represented by the phases $(Ti, Zr)_3SiC_2$, $(Ti, Zr)C$, Al_2O_3 , and $\alpha-Zr$.

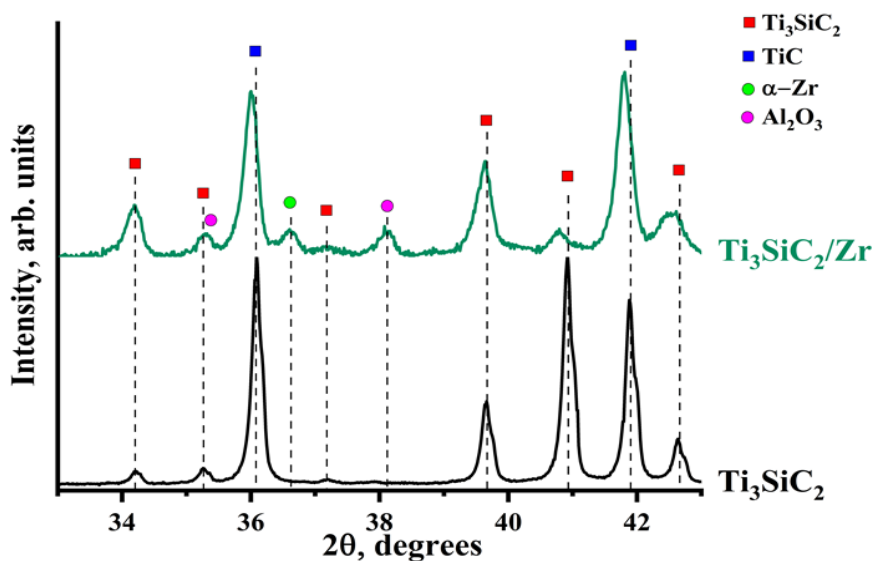


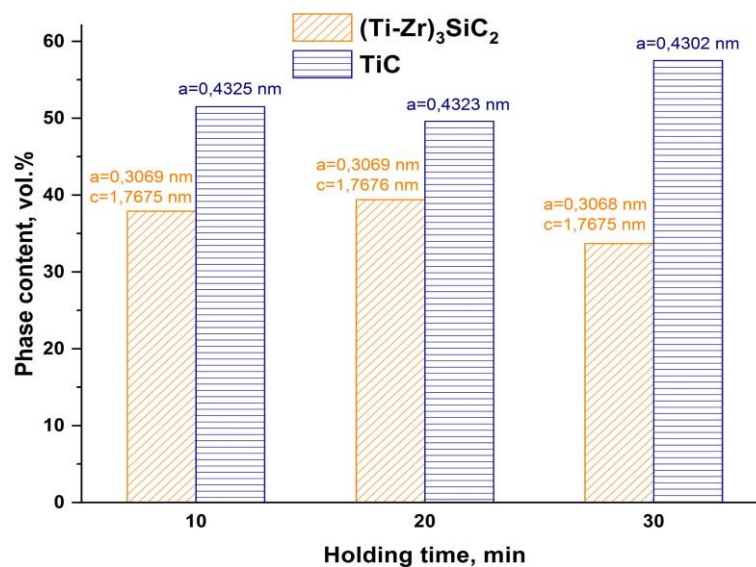
Figure 3. Diffraction pattern of composites based on Ti_3SiC_2 and Ti_3SiC_2/Zr .

Table 1. Results of X-ray diffraction analysis of composites based on Ti_3SiC_2 and $\text{Ti}_3\text{SiC}_2/\text{Zr}$.

Sample	Phase	Phase content, vol. %	Lattice parameters, Å	Coherent scattering region, nm	Microstrain, $\times 10^{-3}$
Ti_3SiC_2	Ti_3SiC_2	35	a=3.068 c=17.674	59	0.9
	TiC	53	a=4.320	74	1.2
	Al_2O_3	12	a=4.758 c=12.997	62	0.6
$\text{Ti}_3\text{SiC}_2/\text{Zr}$	$(\text{Ti, Zr})_3\text{SiC}_2$	46	a=3.066 c=17.692	11	5.9
	$(\text{Ti, Zr})\text{C}$	43	a=4.333	31	1.1
	Al_2O_3	10	a=4.754 c=12.960	45	0.6
	Zr	1	a=3.229 c=5.131	25	2.3

An analysis of the X-ray diffraction results demonstrates that the reflections shift for the MAX-phase and the titanium carbide phase towards smaller angles for the Ti-Zr-Si-C systems. It is caused by the substitution of Ti atoms by Zr atoms in the crystal lattice of Ti_3SiC_2 phase, leading to lattice expansion. Complete dissolution of Zr in the MAX-phase is not observed. Metal zirconium, which does not react with the Ti_3SiC_2 and TiC phase, is represented by the α -Zr phase.

Varying the holding time of the samples during sintering leads to a change in the volumetric content of phases without significant changes in the parameters of the crystal lattice (Figure 4). With a holding time increase from 10 to 20 minutes, slight growth in the content of the MAX-phase is observed (within the error of the method). The sintering for 30 minutes leads to the increase in the content of titanium carbide to 57.5 vol. %.

**Figure 4.** Dependence of the phase ratio for the sintered composites based on the $\text{Ti}_3\text{SiC}_2/\text{Zr}$.

3.3. SEM analysis

The microstructure of the cross-section of composite based on the Ti_3SiC_2 MAX-phases with the addition of Zr, obtained by SPS, is shown on Figure 5.

The cross-section of composites is presented as alternating layers of transition zones with different phase contents and the ratio of M-elements in the structure (Figure 5). There are 4 main zones: the MAX-phase Ti_3SiC_2 with low content of titanium carbide (regions I); zirconium silicide with inclusions of

MAX-phase $(\text{Ti, Zr})_3\text{SiC}_2$ and $(\text{Ti, Zr})\text{C}$ (regions II); $(\text{Ti, Zr})\text{C}$ and MAX-phase $(\text{Ti, Zr})_3\text{SiC}_2$ enriched with zirconium (regions III); Zr phase and $(\text{Ti, Zr})\text{C}$ enriched with zirconium (regions IV).

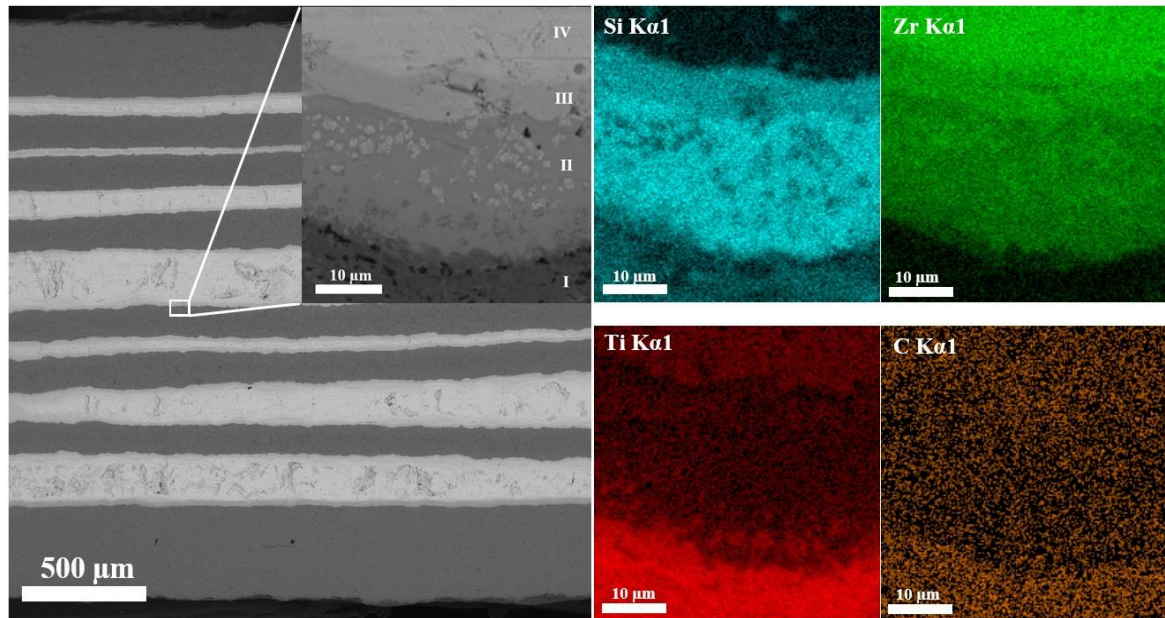


Figure 5. Cross-section SEM images and corresponding EDS maps of the $\text{Ti}_3\text{SiC}_2/\text{Zr}$ based composites sintered at 1400°C , 50 MPa for 10 minutes.

4. Conclusion

The laminated $\text{Ti}_3\text{SiC}_2/\text{Zr}$ based composites were successfully fabricated by SPS using preceramic papers and Zr powder as feedstock. The microstructure of obtained composites is represented by layers of metal zirconium and composite ceramics. It was shown that the layers interact to form a multilayer structure consisting of $(\text{Ti, Zr})_3\text{SiC}_2$, $(\text{Ti, Zr})\text{C}$, Al_2O_3 , and $\alpha\text{-Zr}$ phases. In future work, it is necessary to optimize processing technology to obtain the composites with more uniform layers structure. A more detailed study of the kinetics and interaction processes of the ceramic/metal system is also needed.

Acknowledgments

The research was funded by Russian Science Foundation (grant No. 19-19-00192)

References

- [1] Gao N, Miyamoto Y, Zhang D 2002 *Mater. Lett.* **55**(1–2) 61–66
- [2] Holmquist T, Rajendran A, Templeton D 1999 A Ceramic Armor Material Database (U. S. Army Tank Automotive Research, Development and Engineering Center, Warren, Michigan)
- [3] Ward J, Bowden D, Prestat E, Holdsworth S, Stewart D, Barsoum M W, Preuss M, Frankel P. 2018 *Corros. Sci.* **139** 444-453
- [4] Barsoum M W, Radovic M 2011 *Annu. Rev. Mater. Res* **41** 195-227
- [5] Ghosh N C, Harimkar S P 2012 *Advances in Science and Technology of $M_{n+1}AX_n$ Phases* (Woodhead Publishing) 47-80
- [6] Kashkarov E B, Syrtanov M S, Sedanova E P, Ivashutenko A S, Lider A M, & Travitzky N 2020 *Adv. Eng. Mater.* 2000136
- [7] Sedanova E P, Kashkarov E B, Syrtanov M S, Abdullina K R, Mingazova Y R, Lider A M and Travitzky N 2020 *J. Phys.: Conf. Ser.* **1611** 012007

- [8] Kashkarov E B, Pushilina N S, Syrtanov M S, Krotkevich D G, Gotman I, Travitzky N 2021 *Scr. Mater.* **194** 113696
- [9] Bai Yu, Sun M, Cheng L, Fan S 2019 *Ceram. Int.* **45**(16) 20977-20982
- [10] Travitzky N, Windsheimer H, Fey T, Greil P 2008 *J. Am. Ceram. Soc.* **91** (11) 3477-92